Available online at www.sciencedirect.com
ScienceDirect
International Journal of Thermal Sciences 46 (2007) 621–636
International Journal of Thermal Sciences
www.elsevier.com/locate/ijts

Parametric analysis of loop heat pipe operation: a literature review

Stéphane Launay [1], Valérie Sartre [2], Jocelyn Bonjour *

Centre de Thermique UMR 5008 CNRS-INSA-Université Lyon 1, Institut National des Sciences Appliquées, Bât. Sadi Carnot, 9 rue de la Physique, 69 621 Villeurbanne cedex, France

Received 25 July 2006; received in revised form 30 October 2006; accepted 10 November 2006

Available online 20 December 2006

Abstract

Loop heat pipes (LHPs) are heat transfer devices whose operating principle is based on the evaporation/condensation of a working fluid, and which use the capillary pumping forces to ensure the fluid circulation. Their major advantages as compared to heat pipes are an ability to operate against gravity and a greater maximum heat transport capability. In this paper, a literature review is carried out in order to investigate how various parameters affect the LHP operational characteristics. This review is based on the most recent published experimental and theoretical studies. After a reminder of the LHP operating principle and thermodynamic cycle, their operating limits are described. The LHP thermal resistance and maximum heat transfer capability are affected by the choice of the working fluid, the fill charge ratio, the porous wick geometry and thermal properties, the sink and ambient temperature levels, the design of the evaporator and compensation chamber, the elevation and tilt, the presence of non-condensable gases, the pressure drops of the fluid along the loop. The overall objective for this paper is to point the state-of-the-art for the related technology for future design and applications, where the constraints related to the LHPs are detailed and discussed.

Résumé

Les boucles diphasiques à pompage capillaire sont des systèmes dont le principe de fonctionnement est basé sur l'évaporation/condensation d'un fluide et qui utilisent les forces de capillarité pour faire circuler le fluide dans la boucle. En comparaison des caloducs, les principaux avantages des boucles diphasiques à pompage capillaire sont une aptitude à vaincre les forces de gravité, lorsque le système est en position défavorable, et une puissance maximale transférable supérieure. La présente étude bibliographique, basée sur les travaux expérimentaux et théoriques les plus récents, a pour but est de comprendre comment différents paramètres influencent le comportement de la boucle. Après un rappel du principe de fonctionnement et du cycle thermodynamique de la pompe, ses limites de fonctionnement sont décrites. Sa résistance thermique et sa puissance maximale transférable dépendent du choix du fluide de travail, du taux de remplissage, de la géométrie et des propriétés thermophysiques de la structure capillaire, de la température ambiante, de la température de la source froide, de la géométrie de l'évaporateur et de la chambre de compensation, de l'élévation et l'inclinaison du système, de la présence de gaz incondensables et des pertes de pression du fluide le long de la boucle. L'objectif de cet article est de présenter l'état de l'art relatif aux influences de divers paramètres sur le fonctionnement des LHPs.

Keywords: Loop heat pipe; Effect of gravity; Wick characteristics; Working fluid; Fluid charge; Pressure drops; Ambient temperature; Heat sink temperature; Design

Mots-clés : Boucle diphasique à pompage capillaire ; Gravité ; Caractéristiques du milieu poreux ; Fluide ; Charge ; Chutes de pression ; Température ambiante ; Température de la source froide ; Géométrie

* Corresponding author. Tel.: +33 (0)4 72 43 64 27; fax: +33 (0)4 72 43 88 11.
E-mail addresses: stephane.launay@insa-lyon.fr (S. Launay), valerie.sartre@insa-lyon.fr (V. Sartre), jocelyn.bonjour@insa-lyon.fr (J. Bonjour).
[1] Tel.: +33 (0)4 72 43 84 91; fax: +33 (0)4 72 43 88 11.
[2] Tel.: +33 (0)4 72 43 81 66; fax: +33 (0)4 72 43 88 11.

1290-0729/$ – see front matter
doi:10.1016/j.ijthermalsci.2006.11.007

Contents

1. Introduction

In the field of electronic industry, the component development is conducted by the increase in performance and the miniaturization of electronic systems, resulting in an increase of the heat dissipation. To insure a high reliability of the component, which is closely dependent on its temperature level, the thermal management of electronics becomes a major challenge. As conduction or air convection cooling systems are no more efficient to transfer such high heat fluxes, alternative cooling techniques have to be used. Among the available techniques, two-phase capillary thermal control devices such as Heat Pipes (HP), Micro Heat Pipes (MHP), Capillary Pumped Loops (CPL), and Loop Heat Pipes (LHP) are specially promising. They are self-circulating devices where heat is removed by phase change and the working fluid is circulated by thermodynamic forces. The first heat pipe was conceived as a "Perkins tube" in 1892. The first CPL was invented by Stenger, whose results where published in 1966. The LHP was developed and tested in 1972 in the former Soviet Union [1]. The development of LHPs was a response to the challenge of the increasing needs of electronic systems, and with the specific demand of aerospace technology, which requires high operational reliability and robustness [2–10]. The two-phase loops offer many advantages over heat pipes [1,11] in terms of operation against gravity, maximum heat transport capability, smooth-walled flexible transport lines, and fast diode action.

The basic distinction between a conventional CPL and a conventional LHP lies in the fluidic and thermal links of the compensation chamber to the evaporator. This distinction has a large impact on the design and operation of the capillary loop [12, 13]. The physical proximity of the reservoir to the evaporator, which are connected by the use of a secondary wick, simplifies the LHP start-up and makes the LHP operation vapour-tolerant. Both contribute to the robustness of the LHP operation under various conditions. The preconditions required for a CPL is a major disadvantage that makes the LHP a good replacing and competing technology. However, the LHP is a complex system, into which thermal and hydrodynamic mechanisms between the various LHP components are strongly coupled. As an example, temperature and pressure dynamic instabilities, such as under- and overshoot, are sometimes experimentally reported after changes in operational conditions (e.g. variations in heat load and sink temperature) [4,14–16]. Under certain conditions, the LHP can even never really reach a true steady-state, but instead displays an oscillating behaviour [17–19]. Such dynamic behaviours can induce various types of failure, like evaporator dry-out, degradation of performance, temperature oscillations, which are not suitable for the thermal control of electronics.

Currently, LHP miniaturization is in the forefront of an extensive research and development to provide cooling solutions to the high heat load/heat flux problem of advanced electronic packaging [20–28]. The constrained space of such applications requires to design specific LHPs. Various models have been developed for the LHP characterization [7,23,29–32]. The steady state models are useful to size new-designed LHPs and to predict LHP performance for various fixed external conditions. All these studies contribute to the improvement of the understanding of LHP operation and help to point out how various parameters may affect their behaviour. In the present paper, an exhaustive review of the parameters affecting the steady-state LHP operation is performed, based on the most recent published experimental and theoretical results. This review is hence to be regarded as an update extension of two previous review ar-

Nomenclature

A	cross-sectional area	m^2	
c_p	specific heat	J kg^{-1} K^{-1}	
G	thermal conductance	W K^{-1}	
H	height	m	
k	thermal conductivity	W m^{-1} K^{-1}	
l	thickness	m	
L	length	m	
L_v	latent heat of vaporization	J kg^{-1}	
LHP	loop heat pipe		
$\dot{m}$	mass flow rate	kg s^{-1}	
M	mass	kg	
Nu	Nusselt number		
NCG	non-condensable gas		
P	pressure	Pa	
Pe	Peclet number		
Q	heat transfer rate	W	
r	radius of curvature	m	
R	thermal resistance	K W^{-1}	
R_p	pore radius	m	
T	temperature	K	
u	velocity	m s^{-1}	
V	volume	m^3	

Greek symbols

α, β	void fraction		
θ	contact angle	degree	
ρ	density	kg m^{-3}	
σ	surface tension	N m^{-1}	

Subscripts

axial	axial
c	cold case
cond	condenser
cap	capillary
cc	compensation chamber
e	evaporator, evaporation
eff	effective
g	gravity
groove	groove
h	hot case
in	inlet of the compensation chamber
l	liquid
max	maximum
pw	primary wick
sat	saturation
sw	secondary wick
t	total
v	vapour
w	wick

ticles by Ku [33] and Maydanik [1]: the former focused on LHP operating characteristics while the latter mainly dealt with LHP designs and applications.

2. LHP theory

2.1. LHP description

The operation of a LHP is based on the same physical processes as those of conventional heat pipes. The LHP consists of a capillary pump (also called evaporator), a compensation chamber (also called reservoir), a condenser, and vapour and liquid transport lines (Fig. 1). Only the evaporator and the compensation chamber contain wicks; the rest of the loop can be made in smooth tubing. The compensation chamber is the largest component (by volume) of the loop and is often an integral part of the pump. It has two mains functions: (i) to accommodate excess liquid in the loop during normal operation, and (ii) to supply the capillary pump wick with liquid at all times. To facilitate the latter function, a secondary wick is set-up between the pump wick and the reservoir. The wick in the evaporator, called "primary wick", is made of fine pores for purpose of developing a high capillary pressure to circulate the fluid around the loop, while the secondary wick is made of large pores for the purpose of managing the fluid flow between the compensation chamber and the evaporator. The secondary wick physically connects the evaporator to the reservoir in order to supply the primary wick with liquid, particularly when

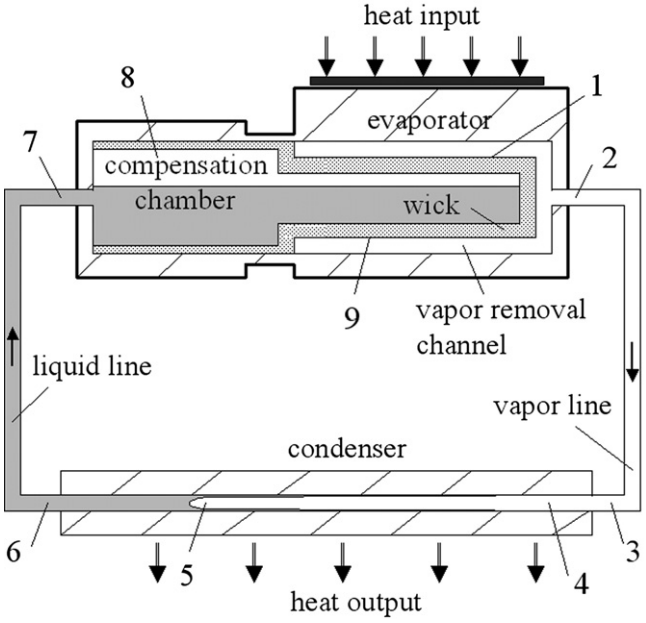

Fig. 1. Geometry of a LHP.

the reservoir is below the evaporator or in microgravity conditions. The heat exchanger, around the condenser line, can be of any type since it can transfer the waste heat efficiently to the sink. Both liquid and vapour lines are made of small-diameter tubing that can easily be arranged in tight spaces around the electronic devices. A portion of the liquid line (called bayonet)

usually first exchanges heat with the reservoir, before it feeds the liquid returning to the capillary pump [34].

2.2. LHP operating principles

The operating principle of the LHP [1,33,35,36] is as follows. Under steady state conditions, for a heat input Q_e supplied to the evaporator, liquid is vaporized, and the menisci formed at the liquid/vapour interface in the evaporator wick develop capillary forces to pump the liquid from the compensation chamber. Since the wick has a finite thermal resistance, the vapour temperature and pressure in the evaporator zone (vapour grooves), which is in contact with the heated evaporator wall, become higher than the temperature and pressure in the compensation chamber. The wick in this case serves as a "thermal lock". At the same time, hotter vapour cannot penetrate into the compensation chamber through the saturated wick owing to the capillary forces which hold the liquid in it (the interface will hold the pressure, preventing any back flow and at the same time providing uninterrupted liquid flow). Thus, another function of the wick is that of a "hydraulic lock". The arising pressure difference causes the displacement of the working fluid around the loop. In this case, three interfaces may exist in the LHP simultaneously: in the evaporator zone, in the condenser and in the compensation chamber. Except in the evaporator, these interfaces may move depending on the heat load, and the excess of liquid is stored into the compensation chamber [1].

A major part $Q_{e,v}$ of the heat input Q_e is used for the liquid vaporization on the outer surface of the primary wick. The vapour generated in the evaporator travels along the vapour line to the heat exchanger where it rejects heat to a sink and turns back to liquid phase. The rest of the heat input, $Q_{e,\mathrm{cc}}$ (called "heat leak") is conducted across the wick and tends to increase the compensation chamber temperature. The amount of heat leak is proportional to the saturation temperature difference between the evaporator and the compensation chamber ΔT_w. ΔT_w is a direct result of the pressure difference across the wick, induced by the vapour, condenser and liquid line pressure drops. The coupling between the pressure drop and the temperature drop across the evaporator wick is responsible for many of the peculiar behaviours found in LHP operation. Thus:

$$Q_e = Q_{e,v} + Q_{e,\mathrm{cc}} \tag{1}$$

$$Q_{e,v} = \dot{m} L_v \tag{2}$$

$$Q_{e,\mathrm{cc}} = G_{e,\mathrm{cc}} \Delta T_w = G_{e,\mathrm{cc}} (T_e - T_{\mathrm{cc}}) \tag{3}$$

where $\dot{m}$ is the mass flow rate, and $G_{e,\mathrm{cc}}$ is the thermal conductance between the evaporator and the compensation chamber. $G_{e,\mathrm{cc}}$ is usually difficult to estimate, all the more since it may depend on the evaporator core state, filled with liquid or not. The effect of the liquid distribution between the compensation chamber and the evaporator core on the LHP performance is discussed in Section 3.

As described above, additional heat going to the compensation chamber tends to increase its temperature. At a specific heat input, an increase in the compensation chamber temperature tends to reduce the two-phase flow length in the condenser. A subcooled liquid flow region will appear before the condenser outlet. Then, the liquid subcooling will compensate a part of the heat leak in the compensation chamber:

$$Q_{e,\mathrm{cc}} = \dot{m} c_{\mathrm{pl}} (T_{\mathrm{cc}} - T_{\mathrm{in}}) \tag{4}$$

where c_{pl} is the liquid specific heat and T_{in} is the liquid temperature at the compensation chamber inlet. At this state, the condenser is divided into three regions: the superheated vapour flow, the two-phase flow and the subcooled liquid flow. The LHP reaches a steady-state operation as the heat leak is totally compensated by the liquid subcooling. The LHP will adjust the saturation temperature until the energy balances for all the loop elements are satisfied. The feedback adjustment of the loop temperature is called "LHP auto-regulation".

2.3. Thermodynamic analysis

A thermodynamic analysis of a capillary two-phase system can help for the understanding of thermal and hydraulic processes in the LHP operation.

A P–T diagram of a working fluid cycle is given in Fig. 2 when the LHP operates at a capillary controlled mode ($P_v > P_{\mathrm{cc}}$). Some details concerning this operating mode are given in Section 3.5. The numbers in the diagram correspond to the physical locations shown in Fig. 1. The vapour generated at the evaporator wick outlet (point 1) is at a saturation state. It becomes superheated at the exit of the grooves (point 2) due to heating and pressure losses. Assuming that the vapour line is perfectly insulated, the vapour temperature drop can be neglected. Since the pressure continues to drop along the way, the vapour becomes more and more superheated relatively to the local saturation pressure until it reaches the entrance of the condenser (point 3). The vapour releases its sensible heat and begins to condense inside the condenser (point 4). The vapour condensation takes place along the saturation line where both the pressure and the temperature decrease. At point 5, the vapour condensation is complete, and the liquid starts to be

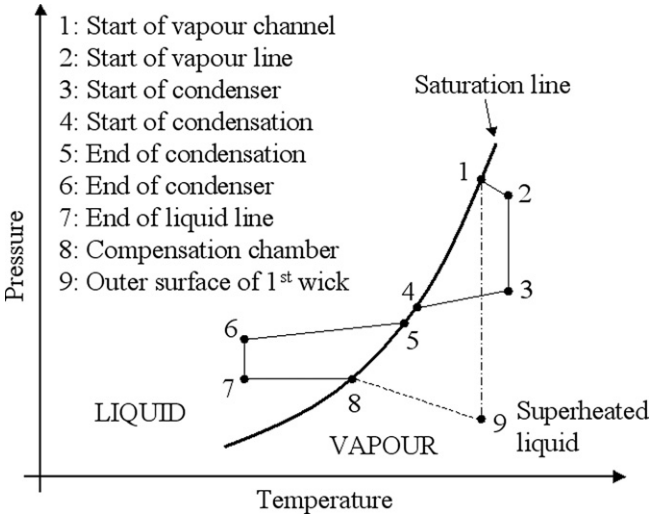

Fig. 2. P–T diagram for LHP steady-state operation (capillary controlled mode) (Chuang [32], Ku [33]).

subcooled inside the condenser until it exits at point 6. The subcooled liquid flows in the liquid line, while its temperature may increase or decrease, depending on whether the liquid looses or gains heat from the ambient. As the liquid reaches the compensation chamber inlet (point 7), the working fluid is heated up to point 8. The liquid subcooling ΔT_{7-8} adjusts itself so that the energy balance of the whole loop is satisfied.

From the thermodynamic states shown in Fig. 2, the following condition must be satisfied for a LHP:

$$P_v - P_{cc} = \Delta P_t - \Delta P_w = (\mathrm{d}P/\mathrm{d}T)(T_v - T_{cc}) \tag{5}$$

where T_v is the saturation temperature of the vapour inside the evaporator grooves (point 1), T_{cc} is the saturation temperature of the fluid in the compensation chamber, and $\mathrm{d}P/\mathrm{d}T$ is the slope of the pressure-temperature saturation line at T_{cc} (point 8). This equation states that, for a given pressure difference between the evaporator and the compensation chamber, a corresponding difference in the saturation temperatures must also exist between the two elements so as to generate exactly the same pressure difference [33].

The evolution from point 8 to 9 corresponds to the liquid flow through the wick into the evaporation zone. On this way, the liquid may be superheated, but boiling does not take place because it remains in such a state for a too short time. Point 9 determines the state of the working fluid in the vicinity of the evaporating menisci, and the pressure drop ΔP_{1-9} corresponds to the value of total pressure losses along the whole loop. It should be noted that, in Fig. 2, the cycle is enlarged to improve its legibility.

2.4. LHP operating limits

Similarly to conventional heat pipes, LHPs are subjected to a number of heat transfer limitations. Due to the various designs of LHPs, these limitations have magnitudes and characteristics different from those of conventional heat pipes [32,36].

2.4.1. Viscous limit

The viscous limitation occurs when the operating temperature is extremely low and the applied heat load is small. It refers to when the viscous forces are larger than the pressure gradients in the heat flow. Under this condition, there is no flow or low flow in the system and the heat transport capability is limited. This situation is usually observed in cryogenic applications or during start-up from a frozen state [32].

2.4.2. Sonic limit

The sonic limit is the maximum allowable mass flow rate or heat transfer that could affect the loop heat pipe operation. The choked vapour flow rate occurs when the vapour reaches the sonic speed. This could happen if the duct cross-sectional area decreases while the working fluid is flowing in the pipe. This would cause the vapour velocity to increase up to sonic speed where the flow would start to choke. Choked flow could occur in a pipe of uniform cross section if the mass flow rate was increased gradually along the axial direction, or if the fluid was accelerated due to phase change in the wick pores [36].

2.4.3. Entrainment limit

In LHPs, since the liquid and vapour flows do not interact the one with the other, this limit is less important than in conventional heat pipes. Nevertheless, some entrainment is likely to occur at the outer surface of the primary wick: in this region, the liquid may be entrained by the high vapour mass flow rate in the channel [32,36].

2.4.4. Capillary limit

For a proper loop operation, the primary wick in the evaporator must have a sufficient capillary pumping head to overcome pressure losses in the loop components [33]. The total pressure drop in the system is the sum of frictional pressure drops in the evaporator grooves, the vapour line, the condenser, the liquid line, and the evaporator wicks, plus any static pressure drop due to gravity:

$$\Delta P_t = \Delta P_{\mathrm{groove}} + \Delta P_v + \Delta P_{\mathrm{cond}} + \Delta P_l + \Delta P_w + \Delta P_g \tag{6}$$

The capillary pressure rise that the wick can develop is given by:

$$\Delta P_{\mathrm{cap}} = P_v - P_l = 2\sigma/r \tag{7}$$

where σ is the surface tension of the working fluid, r is the curvature radius of the meniscus in the wick, and P_l is the liquid pressure under the meniscus at point 9. As the heat load to the evaporator increases, so will the mass flow rate and the total pressure drop in the system. The wick reaches its maximum capillary pumping capability $\Delta P_{\mathrm{cap,max}}$ as $r = R_p/\cos\theta$, where R_p is the pore radius of the wick and θ is the contact angle between the liquid and the wick. Further increase in the heat load will lead to the vapour penetration into the wick and finally to the system deprime. Thus, under normal operation, the following condition must be satisfied all the time:

$$\Delta P_{\mathrm{cap,max}} \geqslant \Delta P_t \tag{8}$$

The pore radius R_p, usually given among the wick characteristics, corresponds to the mean pore radius of the wick. As a wick is usually a heterogeneous material, R_p should correspond to the largest pore radius of the wick [36]. Moreover, especially for cylindrical evaporators, the vaporized mass flow rate may be nonuniform all around the wick outer surface. Then, the capillary limitation may appear in some specific locations, inducing a wick partial dry-out. Consequently, the local heat transfer coefficient at the vaporization area is reduced, but the LHP still operates.

2.4.5. Boiling limit

The evaporator design of LHPs has the ability to tolerate the boiling limit better than heat pipes because heat is conducted from the evaporator body to the primary wick, so that the liquid evaporates at the outer surface of the wick. Boiling may still occur right below the heating surface when the heat load is excessively high. However, the generated vapour bubbles can be vented out to the vapour channel easily [32]. The temperature difference needed for nucleation is given by Dhir et al. [37]:

$$T_l - T_{\mathrm{sat}} = \frac{(2\sigma/R_p - P_{\mathrm{NCG}})T_{\mathrm{sat}}}{\rho_v L_v} \tag{9}$$

According to Kaya and Goldak [38], who have developed a numerical modelling of heat and mass transfer in the capillary structure of a LHP, it is desirable to maintain a very good contact at the fin-wick interface and to eliminate the non-condensable gases in order to increase the boiling limit.

3. LHP parametric study

A parameter study on the LHP operation is difficult as strongly coupled physical mechanisms are involved in LHPs. Each parameter effect has been deduced from theoretical analysis, experimental observations or numerical studies. We should keep in mind that in most of the studies, ammonia is the working fluid. The use of fluids of lower pressure may amplify the sensitivity of the LHP operation to some parameters.

3.1. Effect of fluid charge

The compensation chamber volume V_{cc} must be able to accommodate at least the liquid volume swing (and density changes) between the hot case and the cold case of the loop operation [33]. The fluid inventory must satisfy the following relationships for the cold and the hot cases, respectively:

$$M = \rho_{l,c}\left[V_l + V_{pw} + V_{sw} + V_{groove} + V_v + V_{cond} + (1-\beta)V_{cc}\right] + \rho_{v,c}\beta V_{cc} \quad (10)$$

$$M = \rho_{l,h}\left[V_l + V_{pw} + V_{sw} + (1-\alpha)V_{cc}\right] + \rho_{v,h}[V_{groove} + V_v + V_{cond} + \alpha V_{cc}] \quad (11)$$

where V_l is the volume of the liquid line; V_{pw} and V_{sw} are the void volumes of the primary wick and secondary wick, respectively; V_{groove}, V_v, and V_{cond} are the volumes of the evaporator grooves, the vapour line and the condenser, respectively. β and α correspond to the void fraction of the fluid in the compensation chamber at the cold and hot cases, respectively. β and α are selected at the designer's discretion. Once these values are determined, the compensation chamber volume and the fluid inventory can be calculated from the above equations. At any operating mode of the LHP, both liquid and vapour phases have to coexist in the compensation chamber. Then, it is meaningful to study the fluid charge effect on the LHP performance as long as the compensation chamber is filled with a two-phase fluid.

From the thermodynamic analysis, the fluid charge has no effect on the steady-state LHP performance. However, from the thermal analysis, whether or not the evaporator core contains liquid and/or vapour bubbles may affect the radial heat leak, which has a significant impact on the loop operation. Indeed, the evaporator core may contain liquid or vapour depending on the fluid charge or the LHP position. The presence of vapour bubbles in the evaporator core shortens the heat flow path and significantly increases the heat leak. The evaporator core may act as a heat pipe, transferring efficiently heat from the wick internal surface to the compensation chamber.

Ku et al. [14] have presented an experimental study of a loop heat pipe at low power operation, using ammonia as the working fluid. The fluid inventory and the relative tilt between the evaporator and the compensation chamber were varied so as to create various void fractions in the evaporator core. The test results indicate that the vapour void fraction inside the evaporator core is the most important factor in controlling the loop operation at low heat loads. Consequently, a wick with a low thermal conductivity is highly desirable because it will reduce the heat leak, and hence mitigate the effect of the void fraction. The effect of the heat leak on the LHP operating temperature is presented in Section 3.6.

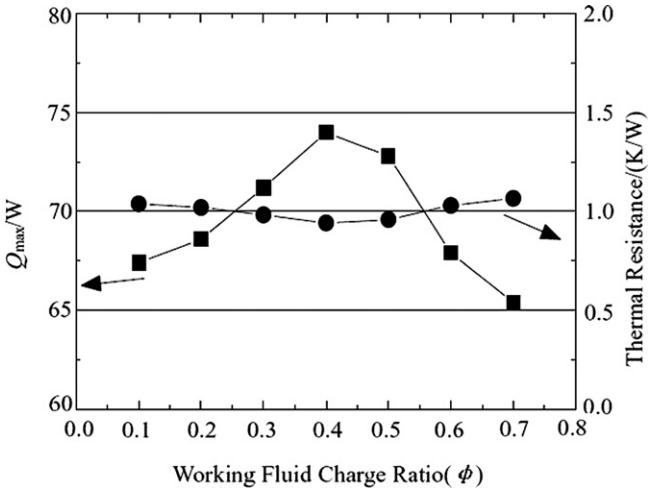

Fig. 3. Q_{max} and R_{th} vs. working fluid fill charge ratio (methanol—1.0 μm LHP for $T_{in} = 20\,^{\circ}C$) (Boo et al. [40]).

Lee et al. [39] have investigated the LHP optimum fill charge ratio and the heat flux conditions, based on experimental measurements at horizontal position. For this specific LHP, the compensation chamber is located above the wick. Thus, the modification of the filling ratio tends to modify the liquid height above the wick. Two kinds of sintered metal wick (stainless steel and brass) have been tested and distilled water was used as the working fluid. The fill charge ratio ranged from 40 vol% to 60 vol% and the imposed heat flux was varied from 1.5 W cm^{-2} to 5.9 W cm^{-2}. Whatever the used sintered metal wick and the imposed heat flux, the best heat transfer performance was measured for the 51.3 vol% filling ratio.

For a similar LHP configuration as Lee et al. [39], but using methanol as the working fluid and a polypropylene (PP) porous wick, Boo and Chung [40] did not observe any significant effect of the fill charge ratio on the LHP thermal resistance (Fig. 3). Nevertheless, the experimental results indicate a maximum heat load for an optimum value of the fill charge ratio of 0.4–0.5. The maximum heat load was characterized by a maximum heater surface temperature of 90 °C, value beyond which the PP wick may be permanently deformed.

Contrarily to the LHP steady-state operation, the LHP start-up is strongly influenced by the fluid charge, and particularly by the fluid distribution in the LHP before starting. Even with the same boundary conditions imposed on a same LHP, drastic random discrepancies of the wall superheat prior to the LHP start-up were experimentally observed [4]. The presence of vapour bubbles/slugs in the evaporator grooves and/or in the evaporator core may modify the heat flux ratio going to the compensation chamber, which affects the temperature evolution in the

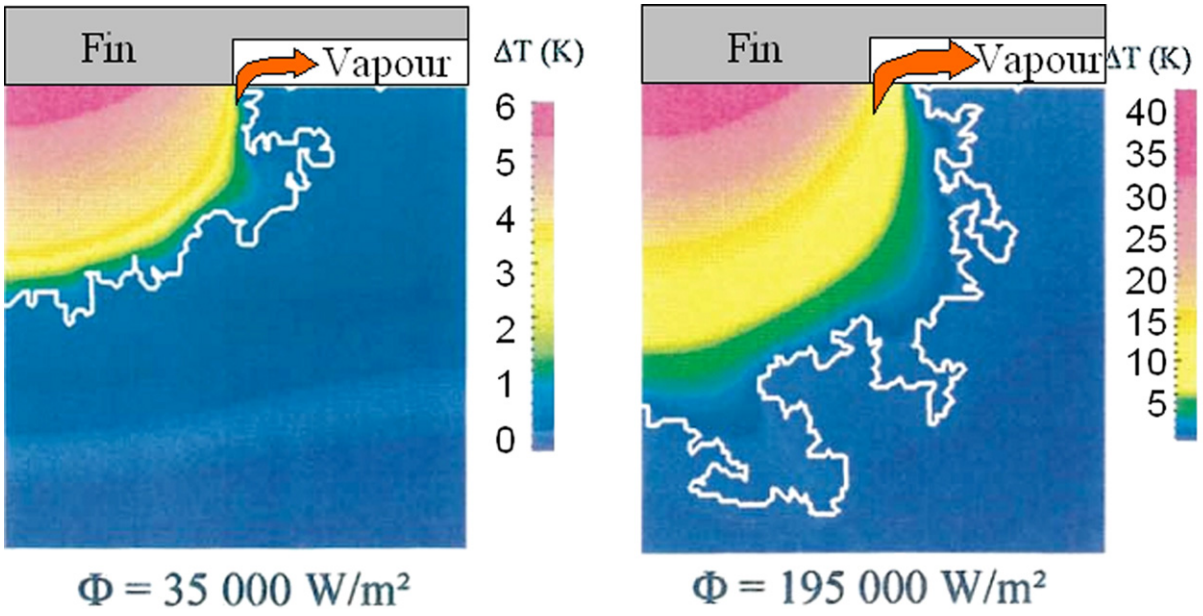

Fig. 4. Temperature fields and liquid–vapour fronts as a function of the heat flux Φ (Figus et al., reprinted from Ref. [43], © (1999) with permission from Elsevier).

evaporator section [4,12,14,33]. The way a LHP starts can have residual effects in its subsequent operation, as a temperature hysteresis [33].

3.2. *Effect of the porous wick characteristics and of the groove design*

The porous wick characteristics, such as the effective thermal conductivity, the pore diameter, the porosity and the permeability, may have a significant effect on the LHP performance. The wick effective thermal conductivity k_{eff} is a function of its porosity and of the wick and liquid thermal conductivities. Considering the LHP theory, the k_{eff} value may affect the radial heat leak and consequently, the LHP operating temperature. The pore diameter and the wick permeability may affect the capillary and boiling limits.

From a detailed analysis of the evaporator wick presented by Mishkinis et al. [41], the radial heat leak by conductive heat transfer across the wick is proportional to the effective thermal conductivity as long as the Peclet number is low. The Peclet number represents the relative magnitude of the convective to the conductive heat transfer and is given by:

$$Pe = \frac{\rho c_p u}{k_{\text{eff}}/l_w} \tag{12}$$

where u is the fluid velocity and l_w is the wick thickness. As the Peclet number increases, a limit exists where the effective thermal conductivity of the wick is no longer the dominant factor. For example, in Teflon wicks, the convective effects are more important than the conductive effects due to the small wick thermal conductivity. According to Hamdan et al. [31], a conductive–convective model of the evaporator wick is necessary for thick wicks with a low thermal conductivity.

The axial heat leak across the evaporator metallic envelope is indirectly affected by the porous medium characteristics, as it depends on the evaporator wall temperature, which is linked to the heat transfer coefficient between the evaporator wall and the evaporation interface in the porous wick. Numerous 2D–3D numerical studies of heat and mass transfer in a capillary structure of a LHP have been conducted [42–45] in order to determine the heat transfer coefficient in the evaporation zone. The heat transfer coefficient is strongly correlated to the vapour front position in the porous structure. Fig. 4 shows the temperature field and the vapour front position in the porous wick calculated for two heat fluxes [43]. From the numerical results, it seems interesting to use a relatively high permeable wick in order to make the vapour flow easier. Platel et al. [46] experimentally observed an increase of the heat transfer coefficient in the evaporation area up to a factor 2.5 when transversal micro grooves machined in the evaporator wall were added to the longitudinal grooves. A parametric analysis has been provided by Yao et al. [45] in order to study the effect of the vapour groove design on the capillary and boiling limits for a LHP. The analysed geometric parameters include the number of grooves, the fin groove width (from 0.15 to 0.65 mm) and the porous wick thickness (from 3 to 8 mm). Calculation results are presented for a sintered nickel porous wick with ammonia as the working fluid. Yao et al. noted that: (1) the boiling limit increases with the number of grooves; (2) the boiling limit is maximum for a fin/groove width ratio of 0.5; (3) the capillary limit increases with the fin width; (4) both the boiling and capillary limits increase as the porous wick thickness decreases. The boiling phenomena first appears in the porous wick located close to the heated fin, where the liquid is at its most superheated state as compared to the liquid distributed in the other part of the porous wick. It could be noted that the boiling limit (around 3 W cm^{-2}) appears at a heat flux one order of magnitude lower than that of the capillary limit (around 60 W cm^2). According to Figus et al. [43], the wick thermal conductivity does not modify significantly the vapour front position in the porous wick, but significantly affects the wall temperature and consequently, the axial heat leak.

Table 1
Characteristics of the capillary porous wicks for the flat evaporator of the LHP test samples (Delil et al. [20])

	LHP 1	LHP 2	LHP 3
Porous wick material	Ni–Cr alloy (X20H80)	Ni	Ti
Thickness [mm]	3.7	7.9	7.3
Maximum pore diameter [μm]	12	2.4	10.4
Porosity [%]	36	66	57
Permeability [m^2]	2.45×10^{-13}	2.45×10^{-14}	2×10^{-13}
Vapour grooves in the contact zone	In the wall of the evaporator body	In the wall of the evaporator body	In the plane of the porous wick

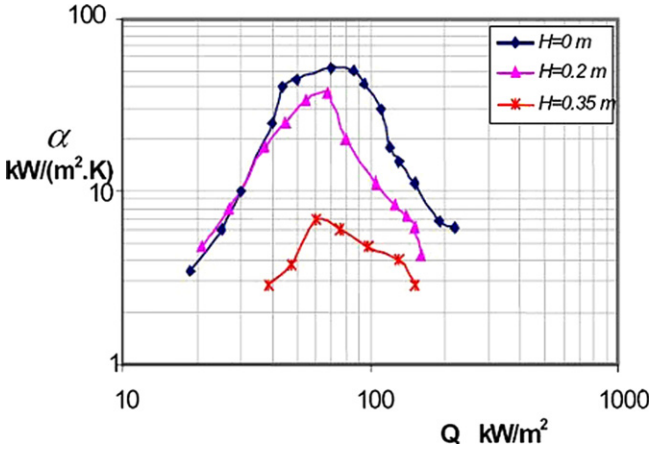

Fig. 5. Heat transfer coefficient α vs. heat flux Q for the LHP1 under a variable height (Delil et al. [20]).

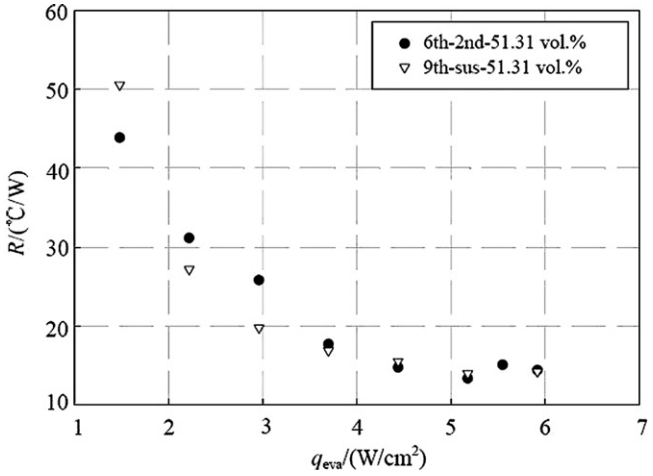

Fig. 6. Thermal resistance as a function of the wick material (2nd: brass—SUS: stainless steel) (Lee et al. [39]).

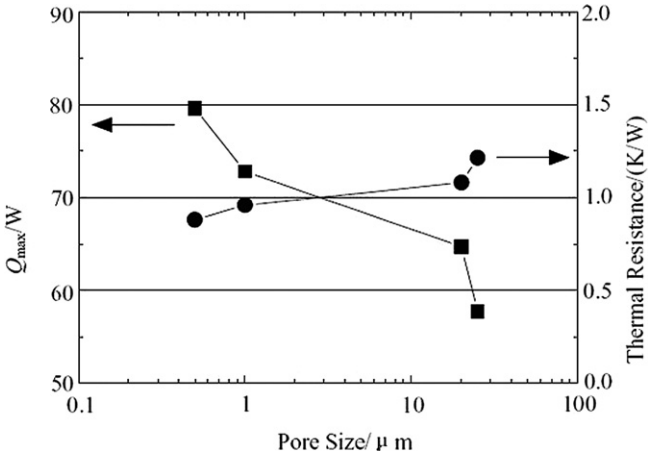

Fig. 7. Q_{max} and R_{th} for various pore sizes of PP wick with methanol and $T_{sink} = 20\,^{\circ}C$ (Boo et al. [40]).

Delil et al. [20] have tested various types of capillary structure in order to define the heat transfer efficiency at the vaporization interface and to study its effect on the LHP performance. The various porous wick characteristics are detailed in Table 1. The heat transfer coefficient for a flat interface between the heating surface and the porous structure has been studied for heat fluxes up to 30 W cm^{-2}. The experimental results for the LHP1 are presented in Fig. 5. At a horizontal position, a maximum heat transfer coefficient of 52 000 W m^{-2} K^{-1} has been measured for the LHP1. Several observations are made: (1) The heat transfer coefficient for vapour grooves machined in the wall of the evaporator body (LHP1 and 2) is higher than for vapour grooves machined in the porous wick (LHP3); (2) A decrease in the maximum pore diameter of the wick considerably increases the potential to operate against a gravitational head; (3) A decrease in the maximum pore diameter in the evaporator shifts the maximum heat transfer coefficient to larger thermal loads. Values of around 80 000 W m^{-2} K^{-1} are quite feasible for ammonia LHPs with cylindrical evaporators [26].

Lee et al. [39] have compared the thermal resistances of two different metal wick LHPs (Fig. 6). The stainless steel powder wick (9th sus) has a porosity of 0.4 with a 9.6 μm effective pore diameter, whereas the sintered brass one (6th–2nd) has a porosity of 0.53 with a 19.1 μm effective pore diameter. The experimental results indicate similar performance, with a small advantage to the stainless steel powder at low heat flux.

Boo and Chung [40] have tested several polypropylene wicks, whose pore diameters ranged from 0.5 to 25 μm. Fig. 7 shows the effect of wick pore size on the maximum heat load and thermal resistance. As the pore size was reduced from 25 μm to 0.5 μm, the maximum thermal load was increased by 45%. At the same time, the thermal resistance of the system was decreased by 33%. A small pore size is recommended when the LHP operates close to the capillary limit. Otherwise, there exists an optimum pore size for which the wick permeability does not damage the evaporator heat transfer coefficient. Similar trends were observed by Liao and Zhao [47], who noticed that the capillary pumping pressure head in the wick structure, with a spherical glass bead diameter ranging from 0.55 to 1.99 mm, was of the same order of magnitude

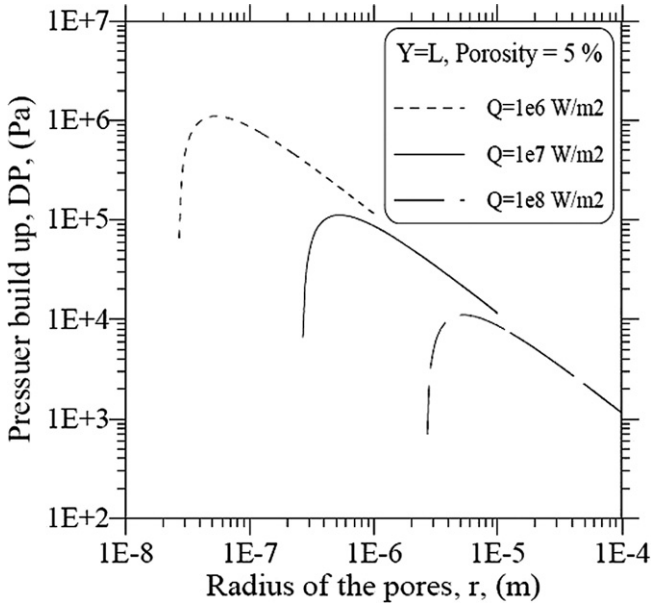

Fig. 8. Pressure across the wick versus pore size for various heat flux (Hamdan [36]).

as the hydrostatic pressure for an elevation ranging from 5 to 50 mm.

The effect of the wick characteristics on the LHP operating limits has been presented by Hamdan et al. [21,31]. Calculation results have been obtained for a coherent porous silicon wick, whose characteristics were imposed by the fabrication technology. Reducing the pore size increases the capillary pressure as $1/R_p$ but at the same time it increases the pressure losses due to friction as Q/R_p^2. So, there exists an optimum value of the pressure build-up across the wick, which depends on the heat flux (Fig. 8). The nucleate boiling limit is correlated to the liquid superheat. A high superheat is desired since it will delay the bubble formation and hence any interface oscillation. As the superheat needed for nucleation is inversely proportional to the pore radius (Eq. (9)), a decrease in the pore radius will increase the boiling limit.

3.3. Effect of the working fluid

Although LHPs were first developed and tested with water or acetone as working fluids for power electronic cooling, most of the detailed results on LHP performance were presented when ammonia was used as the working fluid for the spacecraft thermal control. With the new interest of using LHPs for computer cooling, fluids like water, acetone, methanol or ethanol have been used. The first experimental results showed a significant effect of the working fluid on the LHP performance.

Kaya and Ku [48] have compared the LHP performance by using three different working fluids: ammonia, water and acetone. The model results are shown in Fig. 9. It can be seen that the LHP operating limits are different for each working fluid. The water and acetone LHPs are limited by the absolute vapour pressure at low power levels: the absolute vapour pressure represents the maximum pressure that is available to overcome the total system pressure drops, even when the theoretical capillary pressure head is higher than the total pressure drops. A low pressure corresponding to a fluid temperature near the freezing point severely limits the LHP operation.

While ammonia exhibits many desirable heat transfer characteristics, its freezing point is too high to prevent freezing in the condenser line during a safe mode on a satellite platform. According to Rodriguez and Pauken [49], propylene is a good fluid since it has a lower freezing point and relatively good heat transfer properties. A prototype LHP has been tested with both ammonia and propylene as working fluids. At low sink temperature, the LHP performance was similar for heat loads lower than 100 W (Fig. 10). For higher heat loads, the thermal conductance of the ammonia LHP was approximately four times greater than that of the propylene LHP one.

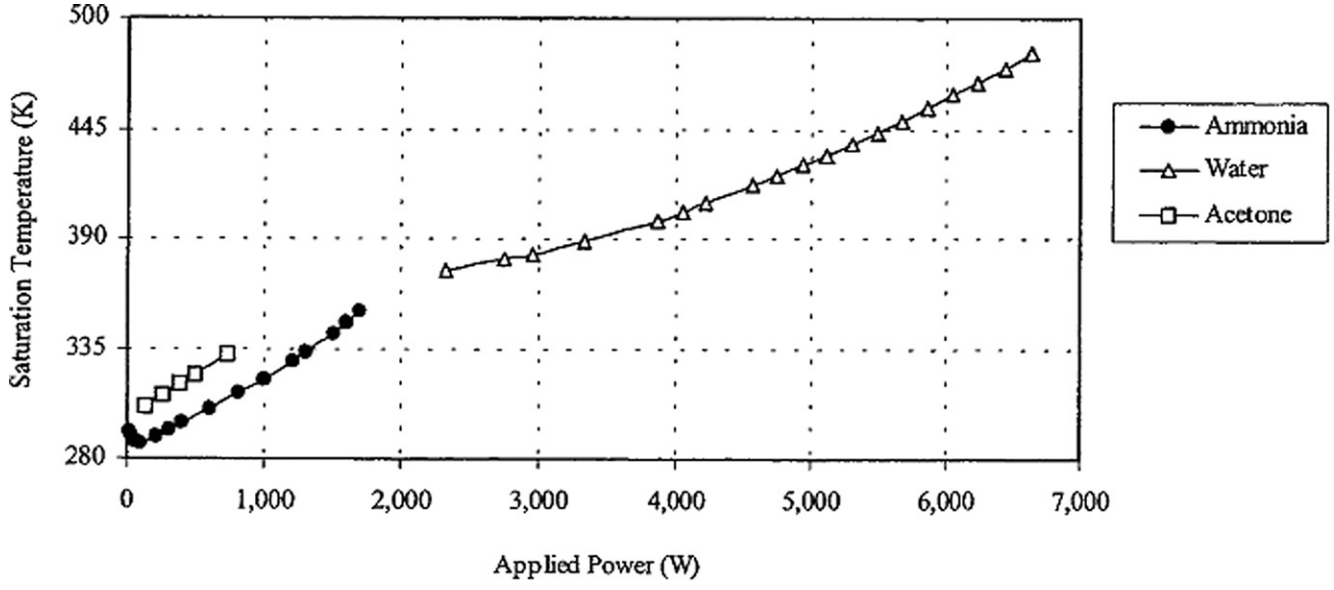

Fig. 9. Effect of the working fluid on the LHP operating temperature (Kaya and Ku [48]). Reprinted with permission from SAE Paper # 1999-01-2006 ©1999 SAE International.

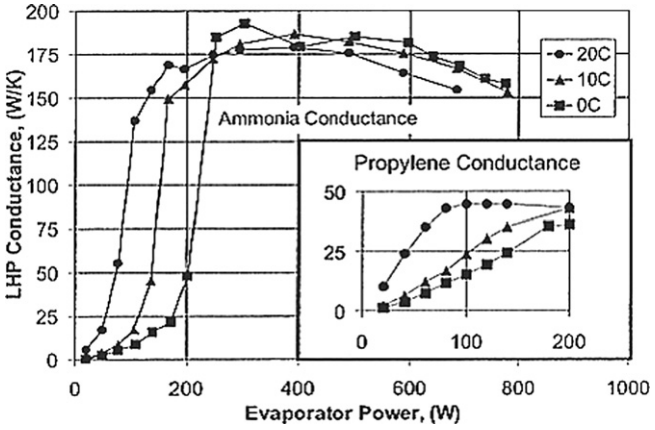

Fig. 10. Comparison of the thermal conductances of ammonia and propylene LHPs (Rodriguez and Pauken [49]). Reprinted with permission from SAE Paper # 2000-01-2317 ©2000 SAE International.

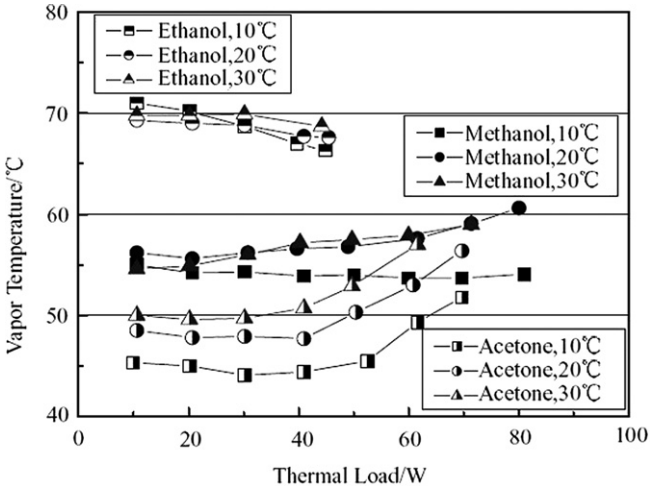

Fig. 11. Vapour temperature variation of the 0.5 μm LHP for three different working fluids under various heat sink temperatures (Boo et al. [40]).

Working fluids including methanol, ethanol, acetone, R134a and water were used by Boo and Chung [40] to compare their performance in a small-scale loop heat pipe containing a polypropylene wick. Methanol, acetone, and ethanol are suitable working fluids for PP-wicks if the temperature remains moderate ($<90\,^{\circ}C$), while R134a and water are incompatible or inappropriate with PP-wicks. At horizontal position, the minimum heat load required for the LHP operation was equal to 10 W for methanol and acetone, and higher than 10 W for ethanol. The LHP vapour temperature variations for three different working fluids under various heat sink temperatures are presented in Fig. 11. For a heat load lower than 60 W, the best performance is obtained for acetone. Methanol was considered as the best working fluid for heat loads higher than 60 W, with a maximum heat load equal to 80 W for heat sink temperatures varying from 10 °C to 30 °C.

According to Baumann and Rawal [8], the liquid thermal conductivity has two significant effects on the LHP performance. Firstly, a low liquid conductivity reduces the heat transfer coefficient in the evaporator, thus limiting the heat transport capability. Secondly, a low liquid thermal conductivity reduces the LHP operating temperature by reducing the wick effective conductivity.

3.4. Effect of non-condensable gases

Unlike heat pipes, LHPs are tolerant to some amount of non-condensable gases (NCGs); however the expected mass of generated gas must be quantifiable. NCGs can be generated for a number of reasons, listed by Ku [33] and Baumann and Rawal [8]. According to Ku [33], the presence of gas in the compensation chamber increases the temperature difference across the wick and consequently, the loop operating temperature.

An experimental study of NCG effects on the LHP operation has been conducted by Nikitkin et al. [50], using ammonia as the working fluid. Tests were performed by injecting various amounts of hydrogen gas into the loop. The results indicated that in large quantities, NCGs increase the start-up time and the operating temperature. The measured effects of NCGs were much smaller than expected, because the gas was absorbed by the working fluid, the envelope and wick materials.

The NCG effects on LHP operation need further investigations, particularly for low pressure working fluids such as water.

3.5. Effect of the gravity (elevation and tilt)

As terrestrial applications of LHPs such as electronic and solar installation cooling are emerging, the effect of gravity needs to be considered carefully. With an additional hydrostatic pressure head, the liquid distribution in the LHP, the two-phase flow and the heat transfer characteristics will vary.

Varying the LHP elevation and tilt are two different ways to study the effect of gravity on the LHP performance. The LHP elevation corresponds to the position of the evaporator with respect to the condenser, while the LHP tilt corresponds to the position of the evaporator with respect to the compensation chamber. An adverse elevation means that the evaporator is above the condenser and an adverse tilt means that the evaporator is above the compensation chamber.

In a gravity environment, a tilt modification will change the fluid distribution, especially between the compensation chamber and the evaporator core. At adverse tilt, the evaporator core may be filled with vapour and consequently, this may increase the LHP operating temperature. Kaya and Ku [51] studied experimentally the performance of a LHP for positive and adverse tilts. The LHP operating temperatures at adverse tilts were much higher than those at positive tilts for low heat loads. At positive tilts, where the evaporator core is completely flooded with liquid, the low steady-state temperatures for low heat loads can therefore be attributed to a substantial reduction of the heat leak and to a more efficient cooling of the compensation chamber, caused by an increase in the mass flow rate. Indeed, at the evaporator outlet, liquid may be pushed by vapour bubbles. The experimental results presented by Chen et al. [19] show that their miniature ammonia LHP (Fig. 12) can work under all test conditions except for adverse tilts. The fact that there is no secondary wick to pump the fluid from the compensation chamber to the primary wick may explain this result.

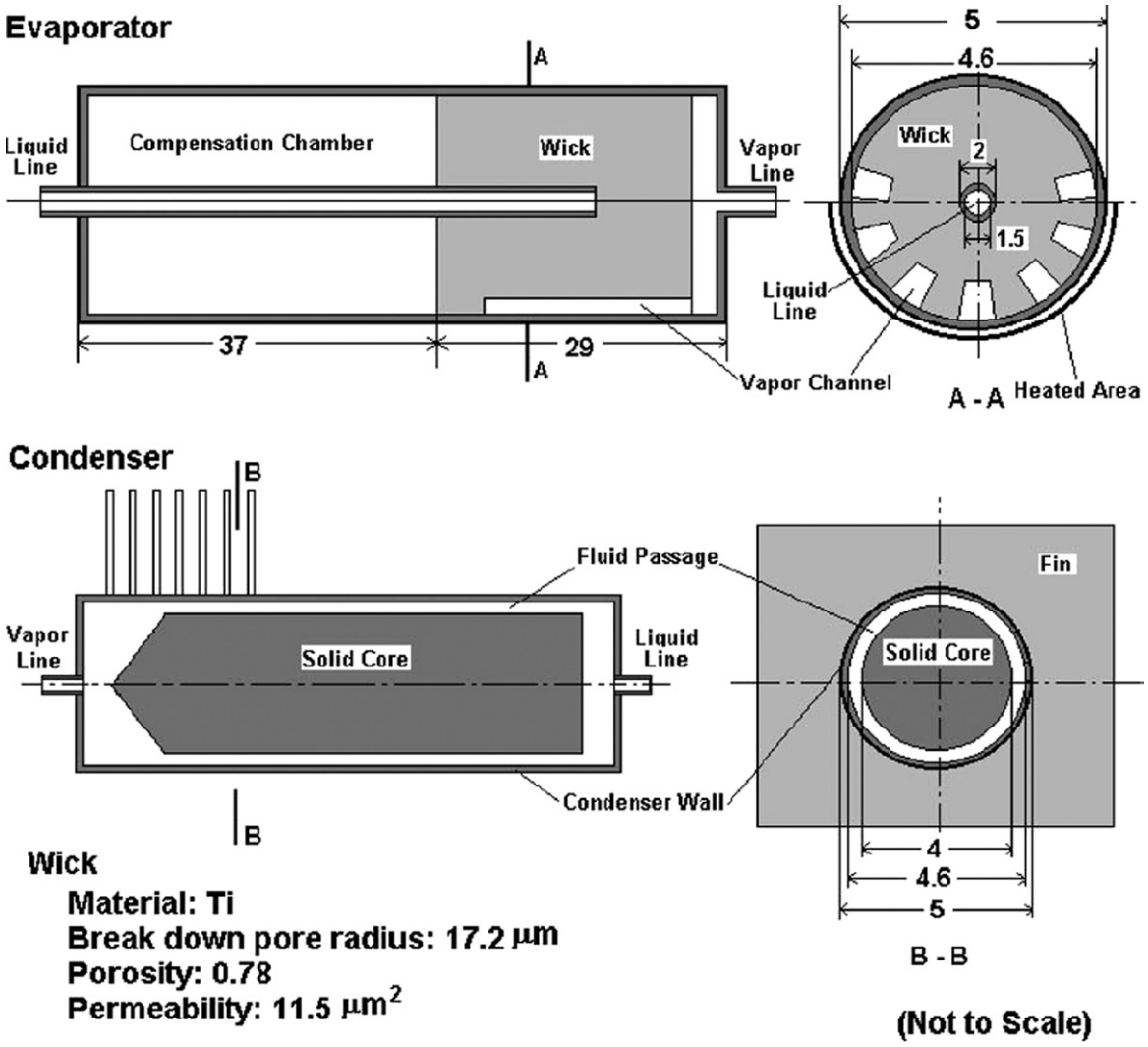

Fig. 12. Schematic of the evaporator and the condenser (Chen et al., reprinted from Ref. [19], © (2006) with permission from Elsevier).

The effect of the relative elevation of the evaporator against the condenser on the LHP performance has been presented by numerous experimental works [19,32,40,48,49,52–54]. All experiments agree well. At low heat loads, adverse elevations tend to increase the LHP operating temperature, compared to the horizontal position, whereas positive elevations tend to decrease it (Fig. 13). The difference in operating temperatures decreases with an increase of the heat load and eventually disappears at large heat loads. Then, for large heat loads, the elevation has usually no effect on the LHP performance.

The operating temperature increase with the elevation has been explained by Ku [33]. As the pressure difference across the wick increases due to gravitational head, the difference in saturation temperatures also increases, which induces an increased heat leak. Since the liquid enthalpy entering to the compensation chamber does not change, the compensation chamber temperature increases in order to provide enough subcooling to compensate for the increased heat leak. At high heat loads, as the gravitational head becomes negligible compared to the frictional pressure drop, the difference in saturation temperatures across the wick is not dependent on the elevation anymore.

Using ammonia [32,53] or propylene [49] as working fluids, with an adverse elevation ranging from 0.05 to 2.7 m, experimental measurements showed an increase of about 50% in the LHP thermal resistance at 20 W. Using acetone as the working fluid [54] and with an adverse elevation of 0.11 m, the thermal resistance was increased by 100% for the same heat load. The experimental results presented by Boo and Chung [40] with a methanol LHP (Fig. 14) have shown a great effect of the gravity on the operating temperature, which vary from 50 °C at the 5 cm-positive elevation to 72 °C at the 10 cm-adverse elevation. It is then clear that the effect of the elevation on the LHP performance is strongly correlated to the working fluid.

Riehl [54] and Chuang [32] have presented some experimental results of the positive elevation effect on the LHP performance, as compared to the horizontal position. The performance improvement is always higher than 50%. Based on experimental measurements, Chuang [32] presented a theory for the LHP operation at a positive elevation. Depending on the source of the pressure driving the system, the LHP can operate in two different modes: capillary-controlled mode and gravity-controlled mode. When the LHP operates in the capillary-

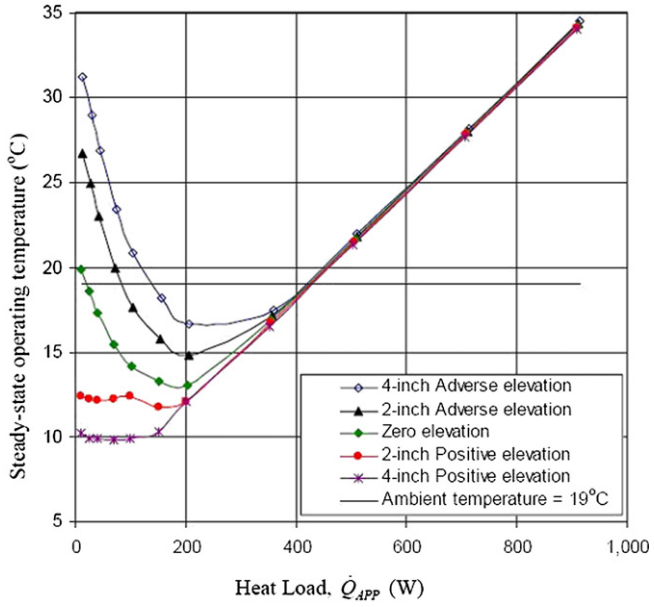

Fig. 13. Effect of the elevation on the steady-state operating temperature ($T_{sink} = 5\,°C$, $T_{amb} = 19\,°C$) (Chuang [32]).

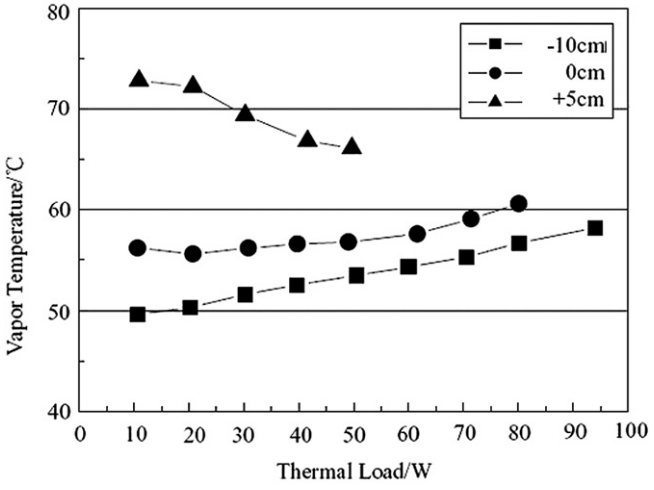

Fig. 14. Effect of the gravity on the vapour temperature variation of the methanol—0.5 μm LHP (Boo and Chung [40]).

controlled mode, the total pressure drops of the system are higher than the net pressure gained from the liquid head. Therefore, the system adjusts the local radius in the primary wick to supply the pressure required to balance the total pressure drops of the system. In this mode, the pressure gained from the liquid head remains at its maximum value. The LHP operates in the gravity-controlled mode when the total system pressure drops are less than the maximum pressure gained from the liquid head. In other words, the pressure gained from the liquid head itself is enough to drive the flow in the system. In this mode, the pores of the primary wick are filled with liquid and there is no meniscus.

From the observations of the test loop using neutron radioscopy, liquid slugs have been observed in the vapour line when the LHP was operated at a positive elevation with small heat loads [32]. Liquid slugs can be easily supported by a smooth vertical tube effortlessly, depending on the tube diameter, the surface tension and the working fluid/wall material contact angle. Pushed by the vapour flow, the liquid slugs travel with the vapour along the vapour line. Then, the total mass flow rate, equal to the sum of the vaporized mass flow rate and the liquid slug mass flow rate, is not proportional to the heat load anymore. This higher mass flow rate tends to reduce the LHP operating temperature.

The effect of gravity on the LHP start-up and on the two-phase heat transfer phenomena in the evaporator and condenser regions may be significant. The effect of gravity on the evaporation heat transfer in the porous wick has been experimentally observed by Delil et al. [20]. The experimental results for the LHP1, whose characteristics are detailed in Table 1, are shown in Fig. 5. Ethanol was used as the working fluid. It is observed that the adverse elevation H has a negative effect on the evaporation heat transfer, which induces a decrease of the LHP performance. Moreover, the effect of H increases with the pore diameter. From the measurements, the evaporation heat transfer coefficient is reduced by a factor 7 for the LHP1 (12 μm pore diameter), for $H = 0.35$ m, whereas it is reduced by only a factor 1.5 for the LHP2 (2.4 μm pore diameter), for $H = 1$ m.

3.6. Effect of the evaporator/reservoir design on the heat leak

The amount of heat leak is composed of two parts: the axial heat leak and the radial heat leak. The axial heat leak refers to the heat conducted from the evaporator metal mass to the compensation chamber through the connection in between. Then, the axial heat leak may depend on the configuration of the compensation chamber, which is connected to the evaporator. The radial heat leak depends on the combination between the thermal and hydrodynamic effects in the porous medium. Detailed calculations of the radial heat leak for cylindrical or flat evaporator can be found in references [23,32,36]. The effects of axial or radial heat leaks were studied independently by Chuang [32]. The axial heat leak term was expressed in [32] as:

$$Q_{\text{axial}} = k_w A \frac{T_e - T_{\text{cc}}}{L} + (k_l \pi L\, Nu) \frac{T_e - T_{\text{cc}}}{2} \tag{13}$$

where the first term is the conductive heat flux and the second term, the convective heat flux in the fluid. The effect of the axial heat leak on the steady-state operating temperature is presented in Fig. 15. The axial heat leak ranges from 0.1 to 20 times the baseline value. The operating temperature increases with an increasing axial heat leak at low heat loads. The reason, mentioned by Chuang [32], is that the axial heat leak dominates the total heat leak when the heat load is small. Similarly, the effect of the radial heat leak on the LHP performance was studied by Chuang [32], by varying the radial heat leak between 0.1 to 5 times the baseline value (Fig. 16). For this parameter study, the radial heat leak is calculated from the conductive heat transfer across the wick. Then, the radial heat leak is proportional to the temperature difference across the wick and is independent of the convective heat transfer between the liquid and the porous medium. The effect of the radial heat leak is important throughout the whole range of heat loads. It can be observed

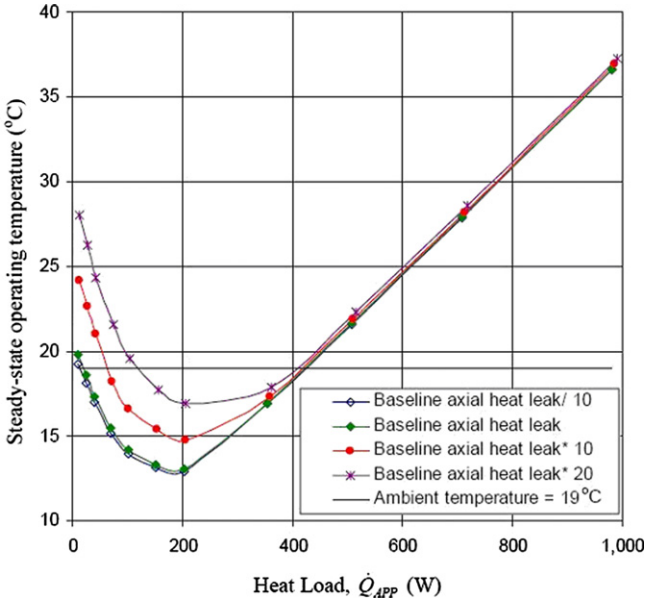

Fig. 15. Effect of the axial heat leak on the steady-state operating temperature ($T_{sink} = 5\,^{\circ}C$, $T_{amb} = 19\,^{\circ}C$, zero elevation) (Chuang [32]).

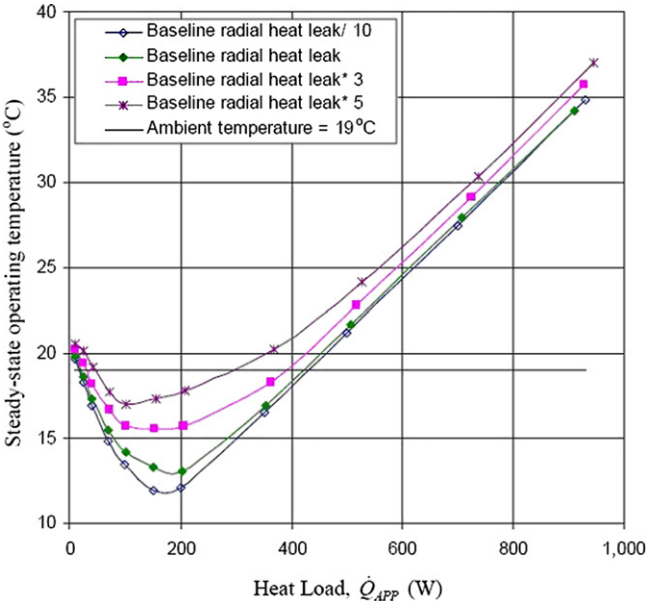

Fig. 16. Effect of the radial heat leak on the steady-state operating temperature ($T_{sink} = 5\,^{\circ}C$, $T_{amb} = 19\,^{\circ}C$, zero elevation) (Chuang [32]).

from Fig. 16 that a higher heat leak leads to a higher steady-state operating temperature.

An experimental investigation of two identical LHPs with different compensation chamber designs was presented by Riehl [55] and by Riehl and Siqueira [56]. The LHP geometries A and B, presented in Figs. 17 and 18, respectively, have the same compensation chamber volume and operate with the same amount of acetone. At steady-state, the LHP A thermal resistance was 4 to 55% lower than the LHP B one. At identical heat loads, the evaporator temperature was higher for the LHP B. Thus, the compensation chamber design determines the fluid distribution between the compensation chamber and the evaporator core. The chamber design also affects the axial heat leak and the heat transfer between the compensation chamber and the ambient, which is in relation to its external surface area.

According to Van Oost et al. [34], the evaporator/compensation chamber design plays a fundamental role on the LHP performance. The compensation chamber and the evaporator have to be thermally disconnected and their hydraulic coupling could be ensured via a secondary wick or a bayonet. The purpose of the bayonet is to vent or directly condense the vapour inside the evaporator core. Advantages and disadvantages of designs with or without bayonet are discussed for LHPs at steady-state and transient operations.

In all parametric studies, axial and radial heat leak effects have been studied independently. However, a variation of the thermal contact between the evaporator metal mass and the wick, caused by a partial wick dry-out at large heat loads (Section 3.2), may modify the LHP typical behaviour.

3.7. Effect of pressure drops

From the LHP theory, the two-phase fluid dynamics between the evaporator and the compensation chamber may impose the temperature difference across the wick, which is used to calculate the amount of heat leak. If liquid and vapour pressure drops in smooth tubes are easily calculated, the two-phase pressure drops are somewhat more difficult to estimate. As an indication, the liquid flow pressure drops are usually small compared to the vapour and two-phase flow pressure drops. For large heat loads, the frictional two-phase pressure drops may represent 60 to 80% of the total line pressure drops [32].

In order to measure the effect of the pressure drops on the LHP operating temperature, an external pressure was imposed on the loop by closing the metering valve on the vapour line at different positions [14]. When tests were performed by applying a constant heat load, it was clearly seen that the loop operating temperature increased as the external pressure drop was increased.

3.8. Effect of sink and ambient temperatures

Heat exchanges (losses or gains) with the ambient around the compensation chamber will modify its energy balance. Heat losses reduce the heat leak and then less subcooling is needed at the reservoir inlet. The reservoir temperature decreases, and inversely for heat gains. Heat exchanges with the ambient along the liquid line will induce an effect similar to the one for the compensation chamber. Indeed, heat gains will tend to increase the liquid temperature between the condenser outlet and the reservoir inlet and then, the liquid subcooling is not sufficient anymore to compensate for the heat leak. The reservoir temperature will then increase. In many applications such as electronic cooling, heat losses to the ambient are not an ideal solution to improve the system efficiency, as maximum of the heat should be removed far from the electronic environment by the condenser.

The effect of the sink temperature on the LHP operating temperature is presented in Fig. 19. For such a study, it is judicious

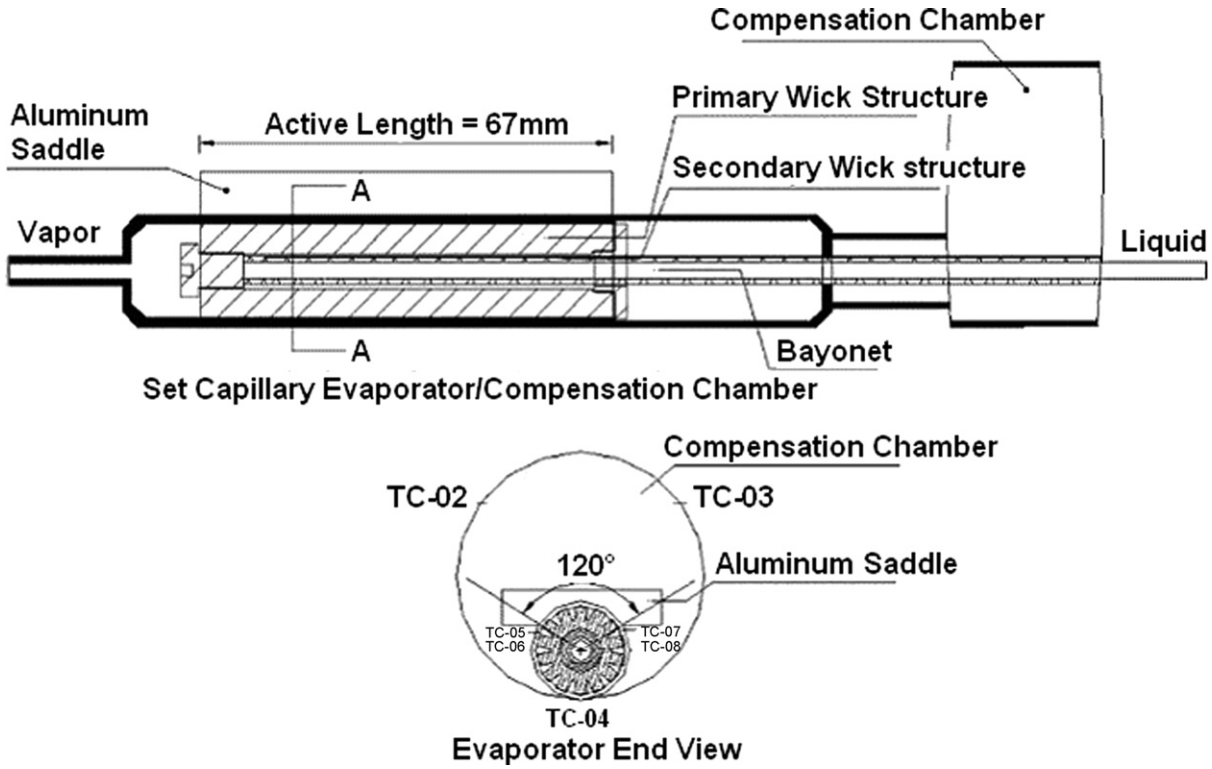

Fig. 17. Evaporator/compensation chamber n° A characteristics (Riehl and Siqueira, reprinted from Ref. [56], © (2006) with permission from Elsevier).

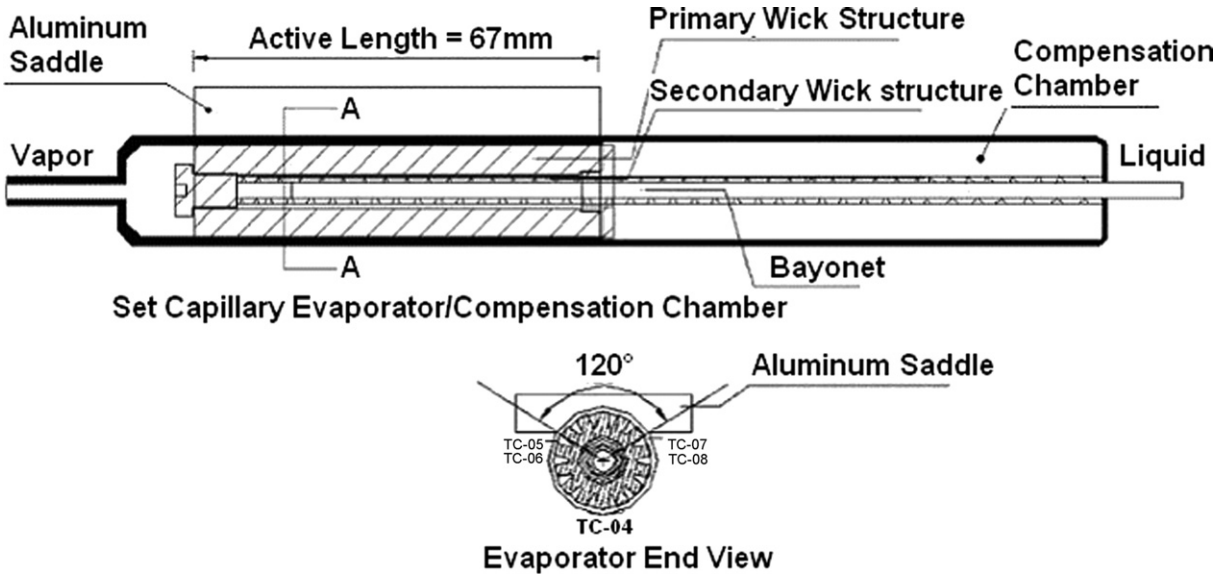

Fig. 18. Evaporator/compensation chamber n° B characteristics (Riehl and Siqueira, reprinted from Ref. [56], © (2006) with permission from Elsevier).

to analyse the evolution of the LHP operating temperature as a function of the temperature difference between the ambient and the sink. A typical U-shaped trend line is observed for large temperature differences. Moreover, we can note that the transition heat load between the variable and fixed conductance modes increases as the temperature difference increases.

Ku et al. [14] have studied the effect of the heat sink temperature on the LHP operating temperature. The test was conducted by cycling the sink temperature between 230 and 290 K while keeping the heat load constant at 5, 25, 50, 100 or 200 W. The compensation chamber temperature did change appreciably with the sink temperature for heat loads of 50 W or higher. As the liquid temperature returning to the compensation chamber varies, the compensation chamber temperature varies too. For lower heat loads, the compensation chamber temperature changed little with the sink temperature, because of the low mass flow rate. As the liquid exited the condenser and flowed along the liquid line, its temperature rose to near the ambient temperature due to parasitic heat gains. Thus, the sink temperature affects the compensation chamber temperature only if it

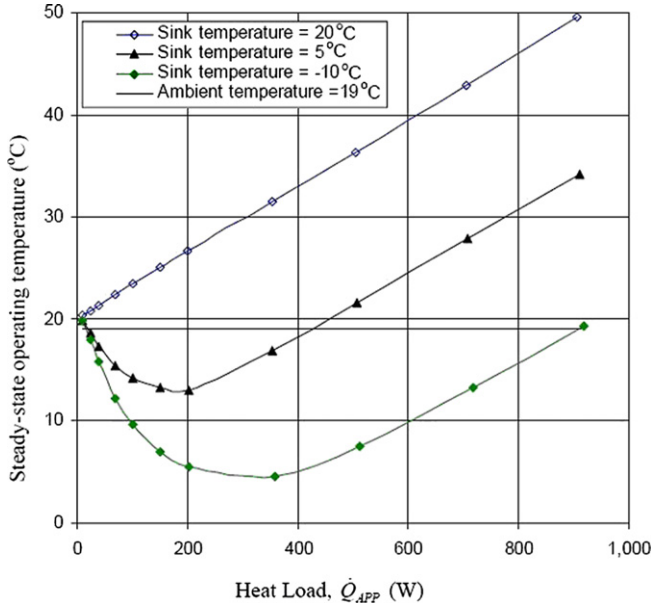

Fig. 19. Effect of the sink temperature on the steady-state operating temperature ($T_{amb} = 19\,°C$ and zero elevation) (Chuang [32]).

affects the temperature of the liquid returning to the compensation chamber.

Any sink or ambient temperature variation may induce an effect on the LHP thermo-hydraulic behaviour, caused by a variation of the fluid thermophysical properties, which are dependent of the temperature. This effect does not seem to have been studied in the literature until now.

4. Conclusions

The LHP performance is characterized by their thermal resistance and maximum heat transport capability. The present literature review has shown that the LHP operation is mainly affected by the boiling and capillary limitations. Providing a parametric analysis is not easy, because the LHP governing parameters are strongly coupled. The fill charge ratio has a significant effect if the void fraction in the evaporator core varies, leading to a radial heat leak variation. The radial heat leak, as well as the ratio of radial to axial heat leak, is affected by the wick characteristics, and the evaporator and compensation chamber designs. The pore size is an important parameter, which should be as low as possible to increase the capillary and boiling limits. The fluid selection mainly depends on its saturation pressure, which should be sufficiently high at the considered operating temperature. Thus, ammonia and propylene are used for low temperature applications; water, alcohols, acetone and R134a may be used for higher temperature applications. In addition, the compatibility of the fluid with the loop materials should be carefully considered. However, the presence of small quantities of NCGs has a weak effect on the LHP operation. The gravity effect is important for terrestrial applications: an adverse elevation or tilt decreases the LHP performance, especially at low heat loads. Likewise, a fluid pressure drop increase tends to decrease the performance. The temperature difference between the ambient and the heat sink affects the transition heat load between variable and fixed conductance modes of the LHP operation.

References

[1] Y.F. Maydanik, Loop heat pipes, Applied Thermal Engineering 25 (5–6) (2005) 635–657.

[2] A.A. Orlov, K.A. Goncharov, E.Y. Kotliarov, T.A. Tyklina, et al., The loop heat pipe experiment on board the GRANAT spacecraft, in: 27th ICES, Noordwijk, The Netherlands, 20–22 May 1997, 13 pp.

[3] C.L. Baker, W.B. Bienert, A.S. Ducao, Loop heat pipe flight experiment, in: International Conference On Environmental Systems, Danvers, July 1998 (SAE paper 981580), 7 pp.

[4] K.-H. Cheung, T. Hoang, J. Ku, T. Kaya, Thermal performance and operational characteristics of loop heat pipe (NRL LHP), in: International Conference On Environmental Systems, Danvers, July 1998 (SAE paper 981813), 9 pp.

[5] D. Douglas, J. Ku, T. Kaya, Testing of the Geoscience Laser Altimeter System (GLAS) prototype loop heat pipe, in: 37th Aerospace Sciences Meeting and Exhibit, Reno, NV, 1999 (AIAA-1999-0473).

[6] M. Amidieu, T. Tjiptahardja, S. Van Oost, B. Mullender, STENTOR CPL: Ground test and modelling results, in: International Conference On Environmental Systems, Toulouse, July 2000 (SAE paper 2000-01-2454), 9 pp.

[7] F. Mena, W. Supper, C. Puillet, Design and development of loop heat pipes, in: International Conference On Environmental Systems, Toulouse, July 2000 (SAE paper 2000-01-2315), 13 pp.

[8] J. Baumann, S. Rawal, Viability of loop heat pipes for space solar power applications, in: AIAA Thermophysics Conference, 35th, Anaheim, CA, 11–14 June 2001 (AIAA 2001-3078), 10 pp.

[9] T.T. Hoang, J. Ku, Advanced loop heat pipes for spacecraft thermal control, in: 8th AIAA/ASME Joint Thermophysics and Heat Transfer Conference, St. Louis, Missouri, 24–26 June 2002 (AIAA-2002-3094), 8 pp.

[10] E. Grob, C. Baker, T. McCarthy, In-flight thermal performance of the geoscience laser altimeter system (GLAS) instrument, in: International Conference On Environmental Systems, Vancouver, July 2003 (SAE paper 2003-01-2421), 11 pp.

[11] D. Bugby, Heat pipe architecture offers flexible thermal control, COTS Journal, July 2005. Available on: http://www.cotsjournalonline.com/home/article.php?id=100367 (consulted on July 11th, 2006).

[12] Y.F. Maydanik, Y.G. Fershtater, Theoretical basis and classification of loop heat pipes and capillary pumped loops, in: 10th IHPC, Stuttgart, Germany, 21–25 September 1997, 15 pp.

[13] M. Nikitkin, B. Cullimore, CPL and LHP technologies: What are the differences, what are the similarities? in: International Conference On Environmental Systems, Danvers, July 1998 (SAE paper 981587), 10 pp.

[14] J. Ku, P. Ottenstein Rogers, K. Cheung, Investigation of low power operation in a loop heat pipe, in: 31st International Conference On Environmental Systems, Orlando, July 2001 (SAE paper 2001-01-2192), 10 pp.

[15] D. Mishkinis, G. Wang, D. Nikanpour, E. MacDonald, T. Kaya, Steady-state and transient loop heat pipe performance during periodic heating cycles, in: 13th IHPC, Shanghai, China, 21–25 September 2004, pp. 71–77.

[16] H.-X. Zhang, T. Ding, X.-G. Shao, G.-P. Lin, R.G. Sudakov, Y.F. Maidanik, Effects of start-up on operating of loop heat pipes, in: 13th IHPC, Shanghai, China, September 21–25, 2004, pp. 133–138.

[17] J. Ku, High frequency low amplitude temperature oscillations in loop heat pipe operation, in: International Conference On Environmental Systems, Vancouver, July 2003 (SAE paper 2003-01-2387), 9 pp.

[18] J. Ku, J.I. Rodriguez, Low frequency high amplitude temperature oscillations in loop heat pipe operation, in: International Conference On Environmental Systems, Vancouver, July 2003 (SAE paper 2003-01-2386), 12 pp.

[19] Y. Chen, M. Groll, R. Mertz, Y.F. Maydanik, S.V. Vershinin, Steady-state and transient performance of a miniature loop heat pipe, International Journal of Thermal Sciences 45 (11) (2006) 1084–1090.

[20] A.A.M. Delil, V. Baturkin, Yu. Friedrikhson, Yu. Khmelev, S. Zhuk, Experimental results on heat transfer phenomena in miniature loop heat pipe with a flat evaporator, in: 12th IHPC, Moscow, 19–24 May 2002, 8 pp.
[21] M. Hamdan, D. Cytrynowicz, P. Medis, A. Shuja, F. Gerner, Loop heat pipe (LHP) development by utilizing coherent porous silicon (CPS) wicks, in: 8th Inter Society Conference on Thermal Phenomena, San Diego, California, 29 May – 2 June 2002, pp. 457–465.
[22] A.A.M. Delil, Y.F. Maydanik, C. Gerhart, Development of different novel loop heat pipes within the ISTC-1360 project, in: International Conference On Environmental Systems, Vancouver, July 2003 (SAE paper 2003-01-2383), 12 pp.
[23] T.T. Hoang, J. Ku, Miniature loop heat pipes for electronic cooling, in: InterPack2003-35245, Maui, Hawaii, USA, 6–11 July 2003, 9 pp.
[24] T. Kaya, J. Ku, Thermal operational characteristics of a small loop heat pipe, Journal of Thermophysics and Heat Transfer 17 (4) (2003) 464–470.
[25] V.G. Pastukhov, Y.F. Maidanik, C.V. Vershinin, M.A. Korukov, Miniature loop heat pipes for electronics cooling, Applied Thermal Engineering 23 (2003) 1125–1135.
[26] Y.F. Maydanik, Miniature loop heat pipes, in: 13th IHPC, Shanghai, China, 21–25 September 2004, pp. 23–35.
[27] C.-C. Hsu, S.-W. Kang, T.-F. Hou, Performance testing of micro loop heat pipes, Tamkang Journal of Science and Engineering 8 (2) (2005) 123–132.
[28] M. Ghajar, J. Darabi, N. Crews, A hybrid CFD-mathematical model for simulation of a MEMS loop heat pipe for electronics cooling applications, J. Micromech. Microeng. 15 (2005) 313–321.
[29] Y.F. Maydanik, Y.G. Fershtater, N. Solodovnik, Loop heat pipes: design, investigation, prospects of use in aerospace technics, SAE Paper 941185, 1994.
[30] T. Kaya, T.T. Hoang, Mathematical modelling of loop heat pipes and experimental validation, Journal of Thermophysics and Heat Transfer 13 (3) (1999) 314–320.
[31] M. Hamdan, F.M. Gerner, H.T. Henderson, Steady-state model of a loop heat pipe (LHP) with coherent porous silicon (CPS) wick in the evaporator, in: 19th Annual IEEE SEMI-THERM, San Jose, California, 11–13 March 2003, 9 pp.
[32] P.-Y.A. Chuang, An improved steady-state model of loop heat pipes based on experimental and theoretical analyses, PhD thesis, The Pennsylvania State University, 2003, 271 pp.
[33] J. Ku, Operating characteristics of loop heat pipes, in: International Conference On Environmental Systems, Denver, July 1999 (SAE paper 1999-01-2007), 16 pp.
[34] S. Van Oost, B. Mullender, G. Bekaert, J.-C. Legros, Secondary wick operation principle and performance mapping in LHP and FLHP evaporators, in: Space Technology and Applications International Forum, Albuquerque, New Mexico, 3–7 February 2002, pp. 94–103.
[35] T.T. Hoang, J. Ku, Heat and mass transfer in loop heat pipes, in: Proc. ASME Summer Heat Transfer Conference, Las Vegas, Nevada, 21–23 July 2003, 9 pp.
[36] M.O. Hamdan, Loop heat pipe (LHP) modelling and development by utilizing coherent porous silicon (CPS) wicks, PhD thesis, University of Cincinnati, 2003, 161 pp.
[37] V. Dhir, S. Kandlikar, Y. Fujita, Y. Iida, R. Heist, Nucleate boiling, in: S. Kandlikar, M. Shoji, V. Dhir (Eds.), Handbook of Phase Change: Boiling and Condensation, 1999, pp. 71–120 (Chapter 4).
[38] T. Kaya, J. Goldak, Numerical analysis of heat and mass transfer in the capillary structure of a loop heat pipe, Int. J. Heat Mass Transfer 49 (2006) 3211–3220.
[39] W.-H. Lee, K.-W. Lee, K.-H. Park, K.-J. Lee, Study on working characteristics of loop heat pipe using a sintered metal wick, in: 13th IHPC, Shanghai, China, 21–25 September 2004, pp. 265–269.
[40] J.H. Boo, W.B. Chung, Thermal performance of a small-scale loop heat pipe with PP wick, in: 13th IHPC, Shanghai, China, 21–25 September 2004, pp. 259–264.
[41] D. Mishkinis, J.M. Ochterbeck, C. Sodtke, J. Ku, D. Butler, Non-dimensional analysis and scaling issues in loop heat pipes in: AIAA Aerospace Sciences Meeting and Exhibit, 41st, Reno, Nevada, 6–9 January 2003 (AIAA 2003-0341).
[42] Y. Cao, A. Faghri, Conjugate analysis of a flat-plate type evaporator for capillary pumped loops with three-dimensional vapor flow in the groove, Int. J. Heat Mass Transfer 37 (3) (1994) 401–409.
[43] C. Figus, Y. Le Bray, S. Bories, M. Prat, Heat and mass transfer with phase change in a porous structure partially heated: continuum model and pore network simulations, Int. J. Heat Mass Transfer 42 (1999) 2557–2569.
[44] T.S. Zhao, Q. Liao, On capillary-driven flow and phase-change heat transfer in a porous structure heated by a finned surface: measurements and modelling, Int. J. Heat Mass Transfer 43 (7) (2000) 1141–1155.
[45] W. Yao, J. Miao, X. Shao, Parametric analysis on LHP/CPL evaporator performance and critical heat flux by two-dimensional calculation, in: 13th IHPC, Shanghai, China, 21–25 September 2004, pp. 125–132.
[46] V. Platel, O. Fudym, C. Butto, P. Briend, Coefficient de transfert, à l'interface de vaporisation, d'une boucle de fluide diphasique à pompage capillaire, Rev. Gén. Therm. 35 (1996) 592–598.
[47] Q. Liao, T.S. Zhao, Evaporative heat transfer in a capillary structure heated by a grooved block, Journal of Thermophysics and Heat Transfer 13 (1) (1999) 126–133.
[48] T. Kaya, J. Ku, A parametric study of performance characteristics of loop heat pipes, in: International Conference On Environmental Systems, Denver, July 1999 (SAE paper 1999-01-2006), 7 pp.
[49] J.I. Rodriguez, M. Pauken, Performance characterization and model verification of a loop heat pipe, in: International Conference On Environmental Systems, Toulouse, July 2000 (SAE paper 2000-01-2317), 7 pp.
[50] M.N. Nikitkin, W.B. Bienert, K.A. Goncharov, Non-condensable gases and loop heat pipe operation, in: International Conference On Environmental Systems, Danvers, July 1998 (SAE paper 981584).
[51] T. Kaya, J. Ku, Ground testing of loop heat pipes for spacecraft thermal control, in: 33rd Thermophysics Conference, Norfolk, VA, 28 June – 1 July 1999, 8 pp.
[52] J.T. Dickey, G.P. Peterson, Experimental and analytical investigation of a capillary pumped loop, J. Thermophysics and Heat Transfer 8 (3) (1994) 602–607.
[53] D.A. Wolf, W.B. Bienert, Investigation of temperature control characteristics of loop heat pipes, in: 24th ICES, Friedrichshafen, Germany, 20–23 June 1994 (SAE paper 941576), 8 pp.
[54] R.R. Riehl, Comparing the behaviour of a loop heat pipe with different elevations of the capillary evaporator, in: International Conference On Environmental Systems, Colorado Springs, July 2004 (SAE paper 2004-01-2510).
[55] R.R. Riehl, Evaluating the behaviour of loop heat pipe with different compensation chamber configurations, in: 13th IHPC, Shanghai, China, 21–25 September 2004, pp. 107–112.
[56] R.R. Riehl, T.C.P.A. Siqueira, Heat transport capability and compensation chamber influence in loop heat pipes performance, Appl. Therm. Engrg. 26 (11–12) (2006) 1158–1168.